



ANALYTIC THEORETICAL ANALYSIS OF THE INCIDENT AND THE REFLECTED SHOCK WAVES APPLIED TO SHOCK TUBES

Bruno Coelho Lima

Faculdade de Tecnologia de São José dos Campos - FATEC Prof. Jessen Vidal - Rodovia Presidente Dutra km 138,7 Eugênio de Melo CEP. 12.247-004 São José dos Campos, SP - Brasil
brunocoelho@ieav.cta.br

Paulo Gilberto de Paula Toro

Alberto Monteiro dos Santos

Instituto de Estudos Avançados, Trevo Coronel Aviador José Alberto Albano do Amarante, nº 1 Putim CEP. 12.228-001 São José dos Campos, SP, Brasil
toro@ieav.cta.br
alberto@ieav.cta.br

Abstract. Shock tubes have been extensively used to investigate many special problems those arise in various fields such chemistry, physics, fluid dynamics, structures and astrophysics. In particular, they have been widely used for high speed and high temperature research since the early 1950s for studies of aerodynamics. Therefore, they are the most versatile experimental short duration ground test facilities, which provide high enthalpy flows close to those encountered during the reentry of a space vehicle into the earth's atmosphere at hypersonic flight speeds. The simplest shock tubes consist basically of a driver and a driven sections, with constant area, separated by a single thin diaphragm. The diaphragm allows one to maintain different pressure in each tube. When the diaphragm is suddenly ruptured at the select high pressure in the driver section, compression waves are generated which coalesce into a normal shock wave. This shock then propagates into the low-pressure driven section while an expansion or rarefaction wave is propagated into the high-pressure driver section. The shock wave arrives at the end wall of the driven section and it is totally reflected. Different gases at different temperatures can be used in the driver and driven sections. The quasi-steady motion may be studied around the model housed in the test section, which is placed at the end or close to the end of the driven section. The one-dimensional incident shock wave moving into a stationary gas and the reflected shock wave mode may be used to calculate the flow conditions in the shock tube and the flow over the test model. The flow modeling of the properties downstream of the shock wave for the simplest shock tube is being presented considering different gases at same initial ambient temperatures used in the driver and driven sections. Theoretical analysis is presented for calorically perfect gas assumption, which the properties downstream of the shock wave are functions only of the flow Mach number, the gas and the properties upstream of the shock wave. Finally, the flow modeling and theoretical analysis for reflected shock wave at the end of the shock tube driven section indicates the possibility to use the high-pressure (stagnation pressure) for hypersonic shock tunnel application.

Keywords: shock tube, hypersonic facility, shock tube modeling, shock tube theoretical analysis

1. INTRODUCTION

In the previous paper (Mantovani et al., 2011) shock tube operation as well as the flow modeling and theoretical analysis for incident shock wave moving into a stationary gas at the low-pressure driven section are presented. Also, it was showing the most important application of the shock tube is to use the quasi-steady motion flow around the model housed placed at the end or close to the end of the driven section for aerodynamics studies and/or for dynamic (pressure transducers and temperature sensors) calibration.

In the present paper, the flow modeling and theoretical analysis for reflected shock wave, which occurs at the end of the shock tube driven section, will be presented and may indicate the possibility to use the high-pressure (reservoir pressure) for hypersonic shock tunnel application.

Shock tubes and shock tunnels are the most versatile experimental short duration facilities. They have been widely used for high velocity and high temperature research since the early 1950s. Both shock tubes and shock tunnels are ground test facilities which provide high enthalpy flows close to those encountered during the reentry of a space vehicle into the earth's atmosphere at hypersonic flight speeds. These short running time facilities require special measurement techniques to measure pressure and temperature (heat flux) for the models in the test section.

Lukasiewicz (1952), Nagamatsu (1958) and Ferri (1961) comment the shock tube was first used by Vielle in France in 1899 to investigate the flame propagation problem. Vielle measured shock velocities up to about twice the velocity of sound in the atmospheric air. From that time, shock tubes have been used extensively to investigate many special problems that arise in various fields such chemistry, physics, fluid dynamics, structures and astrophysics.

The ability of the shock tunnels to simulate the high temperature and velocities of the hypersonic flight has led to its widespread use as a primary tool for high-temperature gasdynamic research applied to hypersonic vehicles design and its components, such as, airbreathing propulsion systems.

The shock tunnel consists of a shock tube with a nozzle attached to the end of the tube to produce higher flow Mach numbers with higher stagnation temperatures in the test section (Nagamatsu, 1958; Ferri 1961).

Since the ability to conduct ground tests at high flight Mach numbers and high enthalpies are limited, expensive flight experiments are also used to design the hypersonic vehicles. An increase in the capability of existing ground test facilities is necessary to reduce the number of required flight tests. Also, the fundamental knowledge necessary for complex flow phenomena at hypersonic flows may be analyzed by the Computational Fluid Dynamic (CFD). But a combination of CFD and experimental investigations that simulate the Mach numbers and the enthalpies for the hypersonic flight conditions is necessary. The experimental data (by ground test facilities and by flight tests) should define the physics of the hypersonic flow phenomena to validate or to modify the available CFD codes.

In the previous work (Mantovani et al., 2011) only the theory of the shock tube was given in some detail in a convenient form to investigate the aerodynamic design of the shock tube and the compressible flow. In this paper, some aspects of shock tube operation are presented to clarify the reflected shock wave modeling flow.

Shock tube consists basically of driver and driven sections, in general with constant cross-section area, separated by a single thin diaphragm, is the most versatile experimental ground test short duration facilities, which provides high enthalpy flows close to those encountered during the reentry of a space vehicle into the earth's atmosphere at hypersonic flight speeds.

When the diaphragm is suddenly ruptured at the select high pressure in the driver section, compression waves are generated which coalesce into a normal shock wave. This shock then propagates into the low-pressure driven section, while an expansion or rarefaction wave is propagated into the high-pressure driver section. Different gases at different temperatures may be used in the driver and driven sections.

After the incident shock wave reaches the closed end of the shock tube wall, the wave is reflected totally. After a while, the reflected normal shock wave interacts with the contact surface. Note that the contact surface separates the compressed and heated gas by the shock wave and the rarefied and cooled gas by the expansion wave and moves right after the incident shock wave, with the same speed u_2 and pressure p_2 of the gas behind the incident shock wave (Mantovani et al., 2011).

2. SHOCK TUBE OPERATION AND MODELING

At $t = 0$ (Fig. 1) thermodynamic properties (pressure, temperature, density), in equilibrium, as well as the velocities of the gases, pressurized in the driver and driven sections, at high pressure p_4 and low pressure p_1 , both gases at ambient temperature $T_4 = T_1$, are identified by the index (4) and (1), respectively.

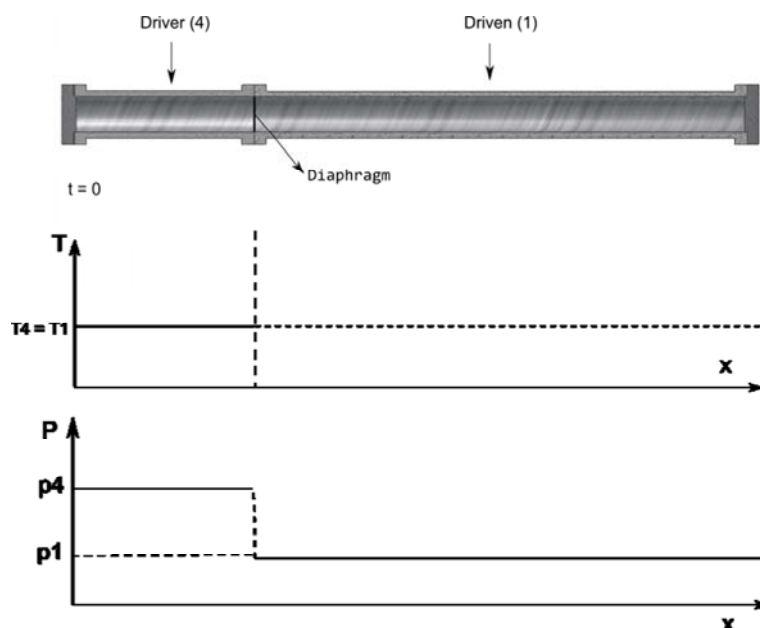


Figure 1: Constant cross section area shock tube, initial conditions for a shock tube.

Ideally, at $t = 0$ (Fig. 2) when the diaphragm is broken, the gas in the high pressure section expands toward the low-pressure section, causing the establishment of a normal shock wave that moves with speed u_s .

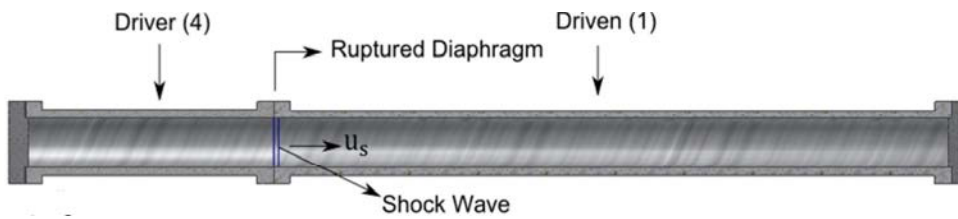


Figure 2: Constant cross section area shock tube right after the rupture of the diaphragm.

At $t = t_1$, As the normal shock wave propagates into the low pressure region (driven section) with velocity u_s (Fig. 3), it increases the pressure of the gas behind the shock wave and induces a mass motion with velocity u_2 . The contact surface between driver and driven gases moves with velocity u_2 and pressure p_2 . The expansion wave propagates to the high pressure region (driver section), smoothly and continuously decreasing its pressure to the lower value p_2 behind the expansion wave.

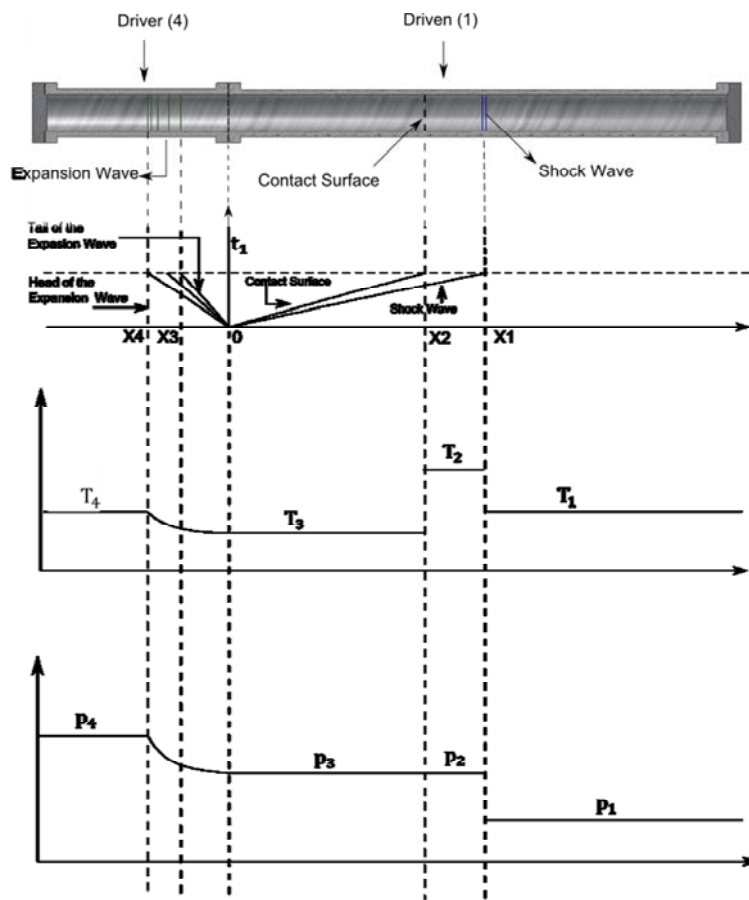


Figure 3: Non-stationary incident normal shock and expansion waves and wave diagram.

The one-dimensional incident shock wave moving into a stationary gas and the reflect shock wave mode (Anderson, 1990; Minucci, 1991; Toro, 1998) may be used to calculate the flow conditions in the shock tube and the flow over the test model (Fig. 2) placed at the end of the shock tube, and the governing flow equations for the one dimensional incident shock wave are given by

$$\text{continuity: } \rho_1 u_s = \rho_2 (u_s - u_2) \tag{1}$$

$$\text{momentum: } p_1 + \rho_1 u_s^2 = p_2 + \rho_2 (u_s - u_2)^2 \tag{2}$$

$$\text{energy: } h_1 + \frac{1}{2} u_s^2 = h_2 + \frac{1}{2} (u_s - u_2)^2 \tag{3}$$

$$\text{equation of state: } h_2 = h_2(p_2, \rho_2) \tag{4}$$

In $t = t_2$, the incident shock wave reaches the closed end wall, of the low pressure section, and the wave is reflected totally (Fig. 4). In $t = t_3$ (Fig. 4), the reflected normal shock wave interacts with the contact surface. The gas between the shock wave and contact surface, from the gas in the low pressure reservoir, induced by the passage of the shock wave, has a constant speed, u_2 , constant pressure, p_2 , constant temperature, T_2 , and constant density, ρ_2 . Consequently, this gas may be used in the study related to high speed flow (gas dynamic research). The useful test time of the gas in the flow conditions (2) is estimated by the interaction of the reflected shock wave with the contact surface.

Once the conditions after the incident shock wave are determined (Eqs. 1-4), the conditions existing in the reflected normal shock wave can be found. The incident shock wave is totally reflected, so $u_5 = 0$ (Fig. 4).

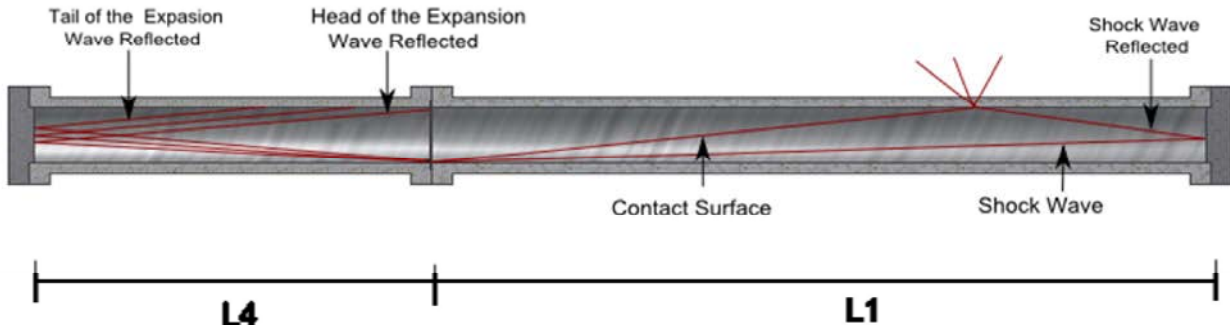


Figure 4: Non-stationary reflected shock and expansion waves.

The governing flow equations, for the one-dimensional reflected shock wave are given by

$$\text{continuity: } \rho_2(u_2 + u_r) = \rho_5 u_r \quad (5)$$

$$\text{momentum: } p_2 + \rho_2(u_2 + u_r)^2 = p_5 + \rho_5 u_r^2 \quad (6)$$

$$\text{energy: } h_2 + \frac{1}{2}(u_2 + u_r)^2 = h_5 + \frac{1}{2}u_r^2 \quad (7)$$

$$\text{equation of state: } h_5 = h_5(p_5, \rho_5) \quad (8)$$

If the conditions achieved in the shock tube are high enough to produce dissociation, ionization or even recombination, the real gas equation must be used; otherwise the calorically perfect gas equation is used, $p = \rho RT$.

3. ANALYTICAL THEORETICAL ANALYSIS

3.1 Incident shock wave analytical theoretical analysis

For the calorically perfect gas assumption the incident (Eqs. 1-4) and the reflected (Eqs. 5-8) shock wave governing equations may be manipulated and one may find the closed analytical solutions (Nagamatsu, 1958; Ferri, 1961; Anderson, 1990; Minucci, 1991; Toro, 1998; Mantovani et al., 2011).

For incident shock wave the closed analytical solutions are given by

$$\frac{p_2}{p_1} = \frac{2\gamma_1 M_s^2 - (\gamma_1 - 1)}{\gamma_1 + 1} \quad (9)$$

$$\frac{T_2}{T_1} = \frac{p_2}{p_1} \frac{\rho_1}{\rho_2} = \frac{[2\gamma_1 M_s^2 - (\gamma_1 - 1)] [(\gamma_1 - 1)M_s^2 + 2]}{(\gamma_1 + 1)^2 M_s^2} \quad (10)$$

$$\frac{\rho_2}{\rho_1} = \frac{(\gamma_1 + 1)M_s^2}{(\gamma_1 - 1)M_s^2 + 2} \quad (11)$$

where the incident shock wave Mach number is given by $M_s = \frac{u_s}{a_1}$ and $\gamma_1 = \frac{c_p}{c_v}$ is the ratio of the specific heats.

The induced velocity imparted by the shock wave moving at constant velocity u_2 may be determined by the continuity condition across the shock wave. Therefore, the induced Mach number, after a moving normal shock wave, is given as function of the incident shock Mach number M_s , and they are given by

$$u_2 = \frac{2}{\gamma_1 + 1} u_s \left(\frac{M_s^2 - 1}{M_s^2} \right) = \frac{2}{\gamma_1 + 1} a_1 \left(M_s - \frac{1}{M_s} \right) \quad (12)$$

$$M_2 = \frac{2(M_s^2 - 1)}{\sqrt{[(\gamma_1 - 1)M_s^2 + 2] [2\gamma_1 M_s^2 - (\gamma_1 - 1)]}} \quad (13)$$

3.2 Shock tube relation

Simultaneously with the instantaneous opening of the diaphragm (between the high and low pressure reservoirs) a rarefaction wave propagates into the high pressure driver tube. Assuming isentropic expansion the pressure ratio in this region is given by

$$\frac{p_4}{p_3} = \left(\frac{a_4}{a_3} \right)^{\frac{2\gamma_4}{\gamma_4 - 1}} \quad (14)$$

The conditions relating the gas states on both sides of the contact surface are that the velocity and pressure are constant across the contact surface. They are given by $u_2 = u_3$ and $p_2 = p_3$. The driver to driven pressure ratio (Shock Tube relation) is given by

$$\frac{p_4}{p_1} = \frac{p_2}{p_1} \left\{ 1 - \frac{a_1(\gamma_4 - 1)}{a_4(\gamma_1 + 1)} \left[M_s - \frac{1}{M_s} \right] \right\}^{\frac{2\gamma_4}{\gamma_4 - 1}} \quad (15)$$

3.3 Reflected shock wave analytical theoretical analysis

After the incident shock wave arrives at the end of the driven tube, the gas is brought to rest, the shock wave is reflected, and the temperature, the pressure and density of the gas after the reflected shock wave are increased (Nagamatsu, 1958; Ferri, 1961; Anderson, 1990, Minucci, 1991; Toro, 1998).

The reflected shock wave produces an induced flow velocity equal and opposite to u_2 in order to bring the gas to rest after the reflected shock wave, given by

$$M_r = -\frac{u_2 - u_r}{a_2} \quad (16)$$

The induced Mach number M_2 after a moving normal shock wave is given as a function of the reflected shock Mach number, given by

$$M_2 = \frac{u_2}{a_2} = \frac{2}{\gamma_1 + 1} \left(M_r - \frac{1}{M_r} \right) \quad (17)$$

The reflected shock Mach number may be written as a function of the incident shock Mach number (Anderson, 1990) as

$$\frac{M_r}{M_r^2 - 1} = \frac{M_s}{M_s^2 - 1} \sqrt{1 + \frac{2(\gamma_1 - 1)}{(\gamma_1 + 1)^2} (M_s^2 - 1) \left((\gamma_1 + 1) \frac{1}{M_s^2} \right)} \quad (18)$$

As one may observe, the reflected shock Mach number M_r is function only of the incident shock Mach number M_s , the ratio of specific heats γ_1 of the existent gas in the driven section (Eq. 18). Also, note the induced Mach number M_2 after a moving normal shock wave is function only of the incident shock Mach number M_s , the ratio of specific heats γ_1 of the existent gas in the driven section (Eq. 13), therefore the reflected shock Mach number M_r may be calculated knowing the induced Mach number M_2 after a moving normal shock wave (Eq. 17).

In both cases the closed analytic solution may be given by

$$\frac{M_r}{M_r^2 - 1} = \frac{M_s}{M_s^2 - 1} \sqrt{1 + \frac{2(\gamma_1 - 1)}{(\gamma_1 + 1)^2} (M_s^2 - 1) \left((\gamma_1 + 1) \frac{1}{M_s^2} \right)} = \frac{2}{(\gamma_1 + 1)} \frac{1}{M_2^2} \quad (19)$$

which may be solve using 2nd degree algebraic equation.

Remembering for the calorically perfect gas assumption the reflected shock wave governing equations (Eqs. 5-8) may be manipulated and one may find the closed analytical solutions.

The thermodynamic properties pressure, density and temperature ratio (related to the pressure, density and temperature behind the incident shock wave) after the reflected shock Mach number are given, respectively, by (Nagamatsu, 1958; Ferri, 1961; Minucci, 1991; Toro, 1998)

$$\frac{p_5}{p_2} = \frac{2\gamma_1 M_r^2 - (\gamma_1 - 1)}{\gamma_1 + 1} \quad (20)$$

$$\frac{T_5}{T_2} = \frac{p_5}{p_2} \frac{\rho_2}{\rho_5} = \frac{[2\gamma_1 M_r^2 - (\gamma_1 - 1)] [(\gamma_1 - 1)M_r^2 + 2]}{(\gamma_1 + 1)^2 M_r^2} \quad (21)$$

$$\frac{\rho_5}{\rho_2} = \frac{(\gamma_1 + 1)M_r^2}{(\gamma_1 - 1)M_r^2 + 2} \quad (22)$$

The thermodynamic properties pressure, density and temperature ratio (related to the pressure, density and temperature across the reflected shock wave) may be obtained as function of the incident Mach number, given by

$$\frac{p_5}{p_1} = \frac{p_5}{p_2} \frac{p_2}{p_1} = \left[\frac{2\gamma_1 M_r^2 - (\gamma_1 - 1)}{\gamma_1 + 1} \right] \left[\frac{2\gamma_1 M_s^2 - (\gamma_1 - 1)}{\gamma_1 + 1} \right] \quad (23)$$

$$\frac{T_5}{T_1} = \frac{T_5}{T_2} \frac{T_2}{T_1} = \left[\frac{[2\gamma_1 M_r^2 - (\gamma_1 - 1)] [(\gamma_1 - 1)M_r^2 + 2]}{(\gamma_1 + 1)^2 M_r^2} \right] \left[\frac{[2\gamma_1 M_s^2 - (\gamma_1 - 1)] [(\gamma_1 - 1)M_s^2 + 2]}{(\gamma_1 + 1)^2 M_s^2} \right] \quad (24)$$

$$\frac{\rho_5}{\rho_1} = \frac{\rho_5}{\rho_2} \frac{\rho_2}{\rho_1} = \left[\frac{(\gamma_1 + 1)M_r^2}{(\gamma_1 - 1)M_r^2 + 2} \right] \left[\frac{(\gamma_1 + 1)M_s^2}{(\gamma_1 - 1)M_s^2 + 2} \right] \quad (25)$$

4. THEORETICAL ANALYSIS RESULTS

As one may observe, for a calorically perfect gas a closed analytical solutions for incident and reflected shock waves may be obtained.

4.1 Incident shock wave analytical theoretical results

The properties downstream of the incident shock wave, considering air as calorically perfect gas: pressure (Fig. 5), temperature (Fig. 6) and density (Fig. 7) ratios across a non-stationary incident shock wave and the Mach number (Fig. 8) behind the incident shock wave (Mantovani et al., 2011) are function only (Eqs. 9-11, 13) of the incident shock Mach number M_s , the ratio of specific heats γ_1 of the existent gas in the driven section and the properties upstream of the incident shock wave (p_1, T_1, ρ_1).

Figures 5 to 7 show as incident Mach number M_s goes to infinite ∞ , the pressure and temperature ratios go to infinite but density ratio approaches to a finite value (6 for air as calorically perfect gas). However, Figure 8 shows the flow Mach number M_2 behind the non-stationary shock wave approaches to 1.89 for air as calorically perfect gas, as incident Mach number M_s increases to infinite ∞ .

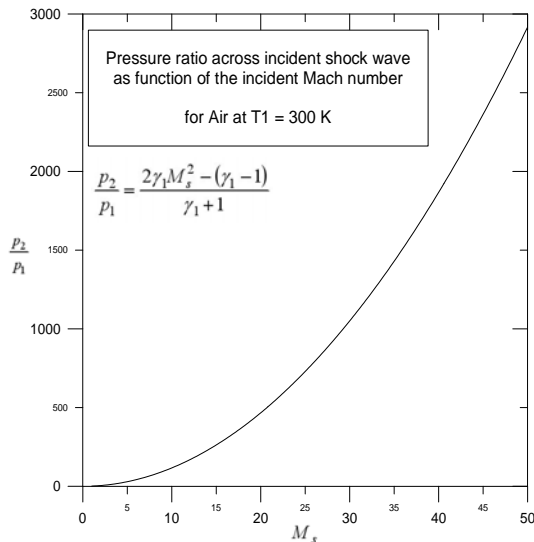


Figure 5: Pressure ratio across incident shock wave.

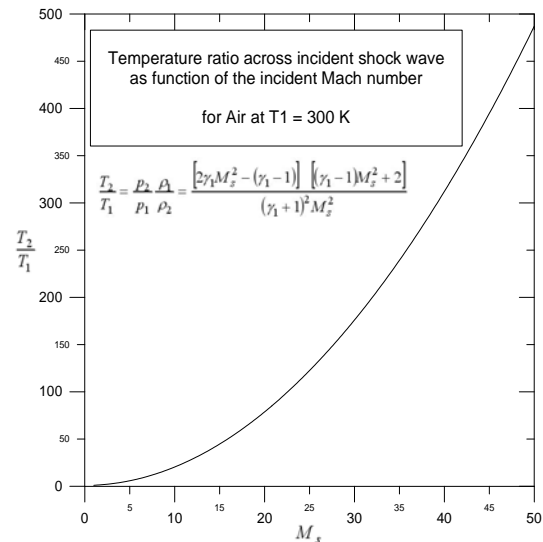


Figure 6: Temperature ratio across incident shock wave.

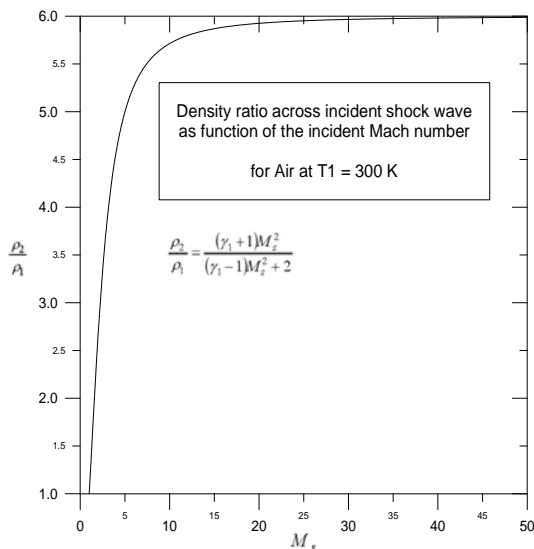


Figure 7: Density ratio across incident shock wave.

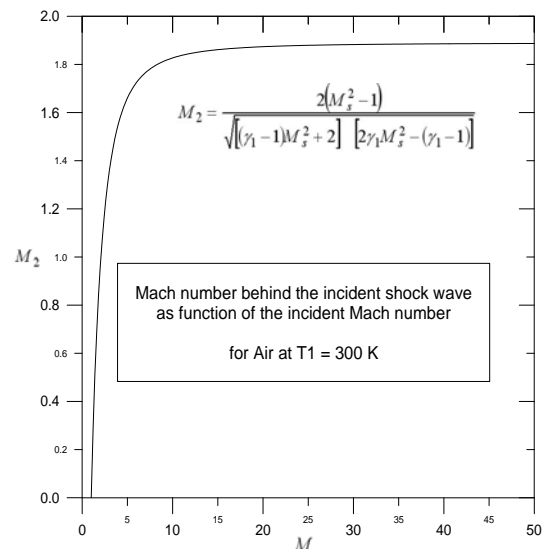


Figure 8: Mach number behind incident shock wave.

Also, experimental investigations using calorically perfect air gas in the driven section of the constant-area shock tubes is possible only at low supersonic flow Mach numbers (behind the normal shock wave). The shock tube technique is limited to the flow Mach number that can be attained in the heated gas between the shock wave and the contact surface. For a diatomic gas (air) with a constant value for the ratio of the specific heats γ_1 of 1.4, the limiting flow Mach number after the incident shock wave is only 1.89 (Nagamatsu, 1958; Ferri, 1961; Anderson 1990; Montovani et al., 2011).

For high-temperature conditions produced by the strong shock waves (about Mach numbers higher than 7 or a velocity higher than 2 km/s, Anderson, 1990), the equations must be modified to include the real gas effects, given by the Eqs. (4) and (8), for incident and reflected shock waves (Nagamatsu, 1958; Ferri, 1961).

4.2 Shock tube relation analytical theoretical result

Finally, by knowing the initial conditions of the gas in the driver and driven sections, the driver to driven pressure ratio (diaphragm pressure ratio), p_4/p_1 , determines the strengths of the incident shock and the expansion waves that are established after the diaphragm is broken.

When the driver is pressurized with air and for a very high driver to driven pressure ratio, p_4/p_1 , the maximum incident shock wave Mach number reach to approximately 6 (Fig. 9).

For a given calorically perfect gas at the driven section, higher driver temperature or low-molecular-weight driver gas than the driven gas maximizes the incident shock strength.

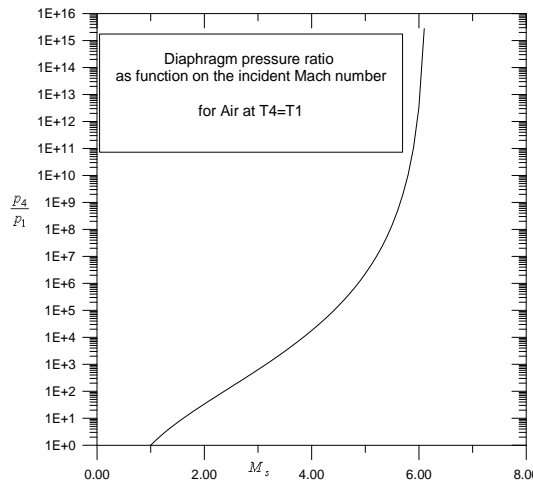


Figure 9: Pressure ratio across incident shock wave.

4.3 Reflected shock wave analytical theoretical results

The properties downstream of the reflected shock wave, considering air as calorically perfect gas: pressure (Fig. 10), temperature (Fig. 11) and density (Fig. 12) ratios across a non-stationary incident shock wave and the reflected Mach number (Fig. 13) are function only (Eqs. 23-25, 19) of the incident and reflected shock Mach number M_s , the ratio of specific heats γ_1 of the existent gas in the driven section and the properties upstream of the incident shock wave (p_1 , T_1 , ρ_1).

Figures 10 to 12 show as incident Mach number M_s goes to infinite ∞ , the pressure and temperature ratios go to infinite but density ratio approaches to a finite value (approximately 20 for air as calorically perfect gas). However, Figure 13 shows the flow Mach number M_r approaches to approximately 6 for air as calorically perfect gas, as incident Mach number M_s increases to infinite ∞ .

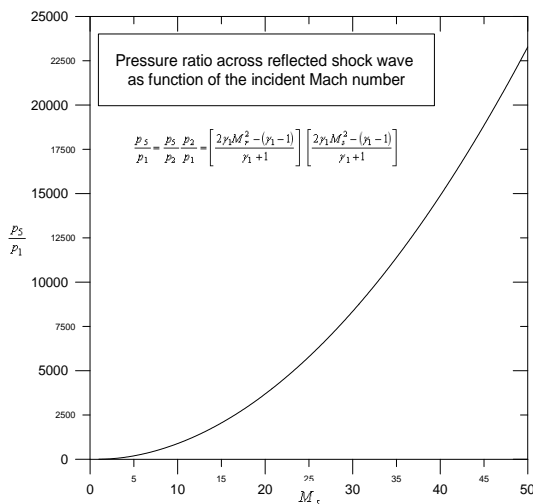


Figure 10: Pressure ratio across reflected shock wave.

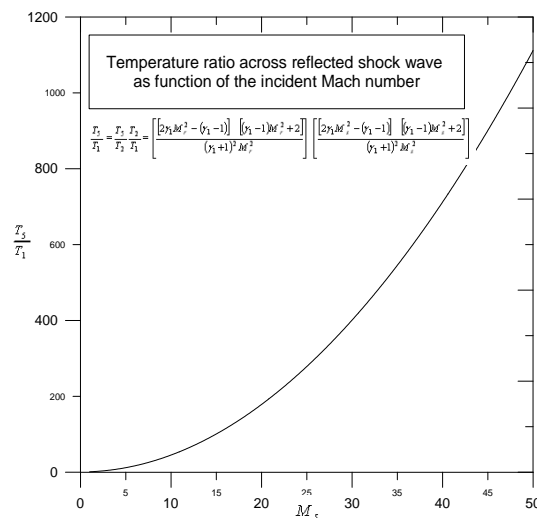


Figure 11: Temperature ratio across reflected shock wave.

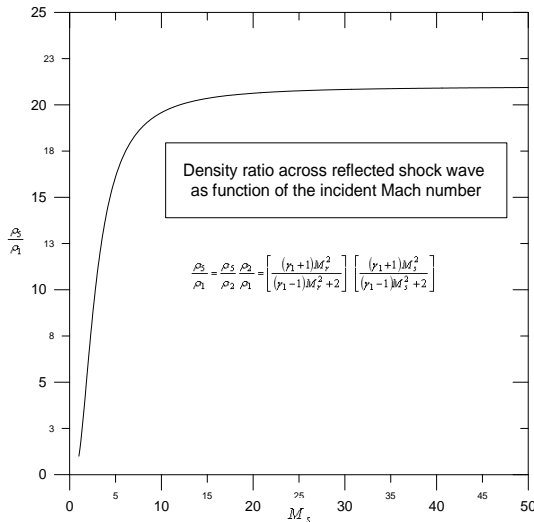


Figure 12: Density ratio across reflected shock wave.

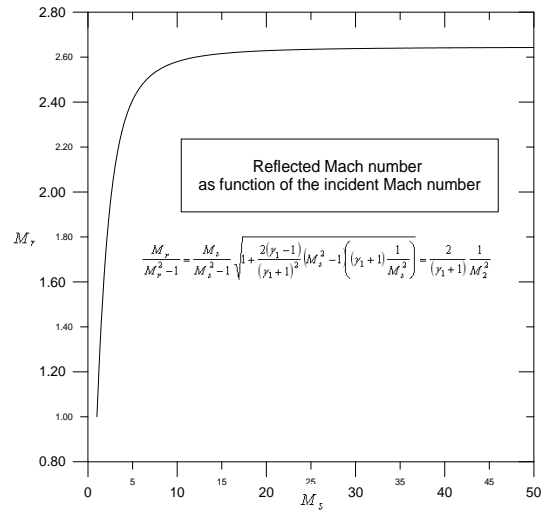


Figure 13: Mach number across reflected shock wave.

5. HYPERSONIC SHOCK TUNNEL APPLICATION

As mentioned earlier, the reflected shock wave at the end of the shock tube driven section indicates the possibility to use the high-pressure (stagnation pressure) for hypersonic shock tunnel application.

Replacing the closed end wall of the low pressure section (Fig. 1) by a convergent-divergent nozzle (Fig. 14) and for a given gas combination with an initial pressure ratio $\frac{p_4}{p_1}$ and an initial temperature ratio $\frac{T_4}{T_1}$, the shock wave strength (M_s or $\frac{p_2}{p_1}$) at the low pressure section (of the shock tube) reaches a finite pressure ratio $\frac{p_5}{p_1}$ and temperature ratio $\frac{T_5}{T_1}$, available to expand in a convergent-divergent nozzle to high temperature (enthalpy) flows close to those encountered during the reentry of a space vehicle into the earth’s atmosphere at hypersonic flight speeds.

Due to the presence of the nozzle throat, the incident shock wave is only partially reflected and the transmitted shock wave disrupts the flow in the nozzle. As a consequence, there exists a finite subsonic velocity u_5 imparted to the flow between the reflected wave and the nozzle inlet. The choked flow at the nozzle throat is assumed (Romanelli Pinto et al., 2011).

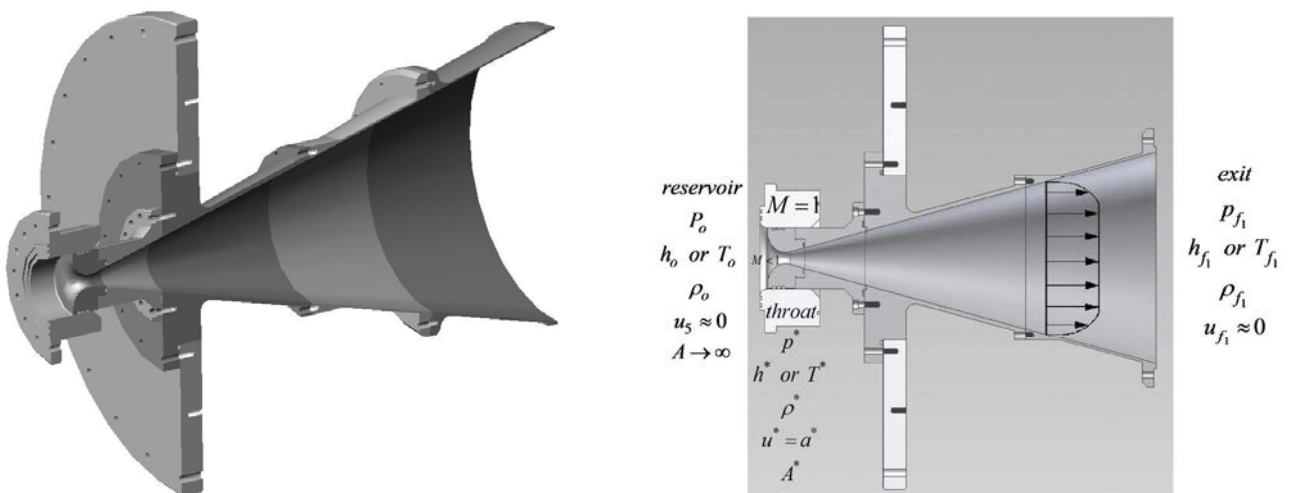


Figure 14: Schematic for subsonic-supersonic (hypersonic) isentropic flow through variable-area ducts (convergent-divergent nozzle) (Romanelli Pinto et al., 2011).

The flow at the inlet of the nozzle comes from the compressed test gas (from the driven section, reservoir, of the Shock Tube). The flow expands isentropically to supersonic (hypersonic) speeds at the nozzle exit, and the high stagnation enthalpy of the oncoming flow is converted into a freestream high speeds in the test section.

The governing flow equations for the one-dimensional reflected shock wave with reflected nozzle (Figs. 4 and 16) are given for reflected shock wave flow by (Minucci, 1991; Toro, 1998; Romanelli Pinto et al., 2011)

$$\text{continuity: } \rho_2(u_2 + u_r) = \rho_5(u_r + u_5) \quad (26)$$

$$\text{momentum: } p_2 + \rho_2(u_2 + u_r)^2 = p_5 + \rho_5(u_r + u_5)^2 \quad (27)$$

$$\text{energy: } h_2 + \frac{1}{2}(u_2 + u_r)^2 = h_5 + \frac{1}{2}(u_r + u_5)^2 \quad (28)$$

$$\text{equation of state: } h_5 = h_5(p_5, \rho_5) \quad (29)$$

and for nozzle throat flow by

$$\text{continuity: } \rho_5 u_5 A_t = \rho^* a^* A^* \quad (30)$$

$$\text{momentum: } p_5 + \rho_5 u_5^2 = p^* + \rho^* (a^*)^2 \quad (31)$$

$$\text{energy: } h_5 + \frac{1}{2}u_5^2 = h^* + \frac{1}{2}(a^*)^2 \quad (32)$$

$$\text{equation of state: } h^* = h^*(p^*, \rho^*) \quad (33)$$

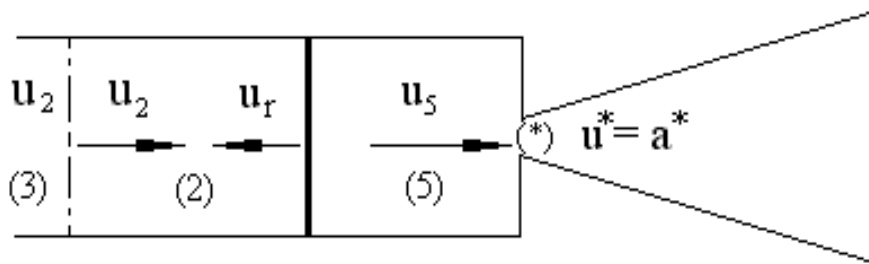


Figure 15: Reflected Shock Wave and Nozzle Entrance.

Once the conditions existing between the first reflected shock wave and the end wall are determined, the stagnation conditions for the model in the test section can be found by the flow in the nozzle in thermodynamic equilibrium (Fig. 16).

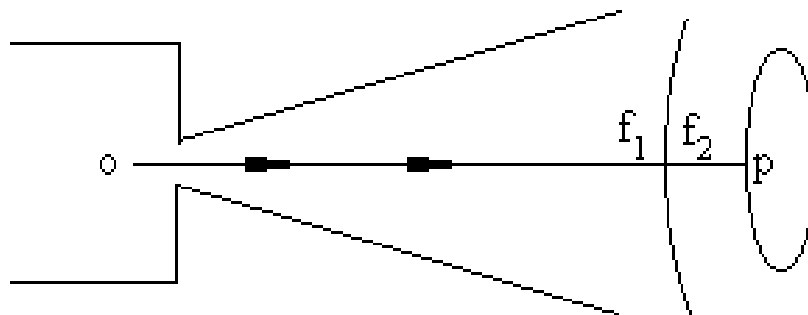


Figure 16: Nozzle Flow.

The flow in the nozzle of the Reflected Hypersonic Shock Tunnel may be assumed in calorically perfect gas. Since the flow expands in the nozzle, the bow normal shock wave is formed in front of the body nose, which is located on the nozzle centerline. The flow in the nozzle expansion is accelerated (upstream) and the flow over the body is decelerated (downstream). In both cases the flow is adiabatic (short duration flow) and isentropic (calorically perfect gas). The flow across the bow shock wave is adiabatic but not isentropic. The inviscid (no boundary layer on the nozzle wall) one-dimensional conservation laws may be used, and they are given by

$$\text{continuity: } \rho_{f1} u_{f1} = \rho_{f2} u_{f2} \quad (34)$$

$$\text{momentum: } p_{f1} + \rho_{f1} u_{f1}^2 = p_{f2} + \rho_{f2} u_{f2}^2 \quad (35)$$

$$\text{energy: } h_{f1} + \frac{1}{2} u_{f1}^2 = h_{f2} + \frac{1}{2} u_{f2}^2 \quad (36)$$

$$\text{equation of state: } h = h(p, \rho) \quad (37)$$

Since the energy is conserved along the streamline, through the shock wave, it may be rewritten as

$$\text{energy: } h_{f1} + \frac{1}{2} u_{f1}^2 = h_{f2} + \frac{1}{2} u_{f2}^2 = h_o \quad (38)$$

and in addition, the isentropic flow upstream (in the nozzle expansion) and downstream (ahead) of shock wave are, respectively, given by

$$s_{f1} = s_o \quad (39)$$

$$s_{f2} = s_p \quad (40)$$

In thermodynamic equilibrium flow two thermodynamic variables determine the gas state. s_o can be determined from the stagnation (reservoir) conditions h_o and p_o , which are known from the shock tunnel flow modeling h_5 and p_5 . s_p can be determined from the flow at stagnation point of the body, the enthalpy and the pressure, which is experimentally measured by pitot probe.

The equilibrium thermodynamic properties, at high enthalpy stagnation condition, are calculated from real gas equation of state. Minucci (1991) presents the solution for this problem with real gas effects for air. The real gas effects are taken into account by utilizing the tabulated real air properties given by Tannehill and Mugge (1974). For calorically perfect gas, low enthalpy stagnation condition, the non-linear system of equations produce analytical algebraic equations as a function only of Mach number of the shock wave and the properties upstream of the shock wave.

Nagamatsu (1958), Ferri (1961) and Anderson (1990) among many others, present the equations and analyses for this case. Also, Anderson (1990) solved the incident shock wave with real gas by iterative process.

Minucci (1991) presented not only the flow modeling for both cases, the Reflected Shock Wave Mode and the Equilibrium Interface Mode, but he also developed a CFD code to solve the equations.

6. CONCLUSION

Shock tubes have been widely developed since the early 1950s as a powerful laboratory short duration tool to study the high speed and high temperature phenomena in compressible gases.

The shock tube operation, flow modeling and incident and reflected analytical theoretical analysis are presented for the constant area shock tube, which consists basically of driver and driven sections, separated by a single thin diaphragm.

For a calorically perfect air pressure, temperature density ratios across a non-stationary incident shock wave as well as the flow Mach number behind a moving incident shock wave are presented as functions only the incident shock Mach number and the ratio of specific heats of the existent gas in the driven section.

Also, for a calorically perfect air pressure, temperature density ratios across a non-stationary reflected shock wave as well as the flow Mach number behind a moving reflected shock wave is presented as functions only the incident and reflected shock Mach numbers and the ratio of specific heats of the existent gas in the driven section.

Finally, Hypersonic Shock Tunnel may be obtained by replacing the closed end wall at the driven section of the Shock Tube by a convergent-divergent nozzle. For the Hypersonic Shock Tunnel application a one-dimensional governing flow modeling is presented.

7. ACKNOWLEDGEMENTS

The second author would like to express gratitude to FINEP (agreement n° 01.08.0365.00, project n° 0445/07) for the financial support for the 14-X Hypersonic Aerospace Vehicle design and experimental investigations (which include the Shock Tube applications); and to CNPq (project n° 520017/2009-9) for the financial support to undergraduate students.

B. C. Lima, P. G. P. Toro and A. M. Santos
Analytic Theoretical Analysis of the Incident and the Reflected Shock Waves Applied to Shock Tubes

8. REFERENCES

- Anderson Jr., J. A., 1990, "Modern Compressible Flow, The Historical Perspective" McGraw-Hill, Inc., 2nd edition.
- Lukasiewicz, J., 1952, "Shock Tube Theory and Applications". National Aeronautical Establishment, Rept. 15, Otawwa, Canada.
- Mantovani, A. F., Romanelli Pinto D., Toro, P. G. P., Minucci, M. A. S., 2011, "Shock Tube Operation, Flow Modeling and Theoretical Analysis", 21st Brazilian Congress of Mechanical Engineering. October 24-28, 2011, Natal, RN, Brazil.
- Minucci, M.A.S. 1991, "An Experimental Investigation of a 2-D Scramjet Inlet at Flow Mach Numbers of 8 to 25 and Stagnation Temperatures of 800 to 4100 K," Ph.D. Thesis, Rensselaer Polytechnic Institute, New York.
- Nagamatsu, H. T., 1958, "Shock Tube Technology and Design", Report No. 58-RL-2107, General Electric Research Laboratory, Schenectady, New York.
- Ferri, A. 1961, "Fundamental Data Obtained from Shock Tube Experiments", chapter III, "Shock Tube Technology and Design" (Nagamatsu, H. T.), Pergamon Press, 1961.
- Romanelli Pinto D., Marcos, T. V. C., Toro, P. G. P., Minucci, M. A. S., Oliveira, A. C., Chanes Junior, J. B., 2011, "Preliminary Characterization of the Hypersonic Flow in the Test Section of the IEAv T3 Hypersonic Shock Tunnel", 21st Brazilian Congress of Mechanical Engineering. October 24-28, 2011, Natal, RN, Brazil.
- Toro, P. G. P., 1998, "Experimental Pressure and Heat Transfer Investigation over a Directed-Energy Air Spike Inlet at Flow Mach Number of 10 to 20, Stagnation Temperature of 1000K, with Arc Power up to 127 kW, Ph.D. Thesis, Rensselaer Polytechnic Institute, New York.
- Tannehill, J. C.; Mugee, P. H., 1974, "Improved Curve Fits for the Thermodynamic Properties of Equilibrium suitable for Numerical Computation using Time-Dependent or Shock-Capturing Methods," NASA CR 2470.

9. RESPONSIBILITY NOTICE

The authors are the only responsible for the printed material included in this paper.
Copyright ©2013 by P. G. P. Toro. Published by the 22nd Brazilian Congress of Mechanical Engineering (COBEM).